JMEPEG (2009) 18:490–495
DOI: 10.1007/s11665-009-9381-2

1059-9495/$19.00

Design and Characterization of New Ti-Nb-Hf Alloys

M. González, J. Peña, J.M. Manero, M. Arciniegas, and F.J. Gil

(Submitted September 15, 2008; in revised form January 26, 2009)

Three new Ni-free Ti alloys Ti-16.2Hf-24.8Nb-1Zr, Ti-5.2Hf-31.2Nb-0.4Zr, and Ti-16Hf-36.2Nb-1Zr (wt.%), were designed and produced in order to obtain shape memory and/or low elastic modulus materials for the use in the load transfer implant field. For that, a method based on the molecular orbital theory was implemented to design the three new Ti-Nb-Hf system alloys. A vacuum arc-melted button of each alloy was treated at 1100 °C for 1.5 h and quenched in a mixture of ethanol/water at 0 °C. Finally, the alloys were microstructurally and mechanically characterized. Special attention on studying the elastic modulus and the thermoelastic martensitic transformation was given by means of nanoindentation tests using a Berkovich and a spherical tip, respectively. X-ray diffraction results showed the presence of β-phase in the three studied alloys. Moreover, one of the alloys exhibited reversible phase transformation due to the presence of thermoelastic martensitic α″-plates inside the β-grains observed by transmission electron microscopy. Results showed a low elastic modulus in all the studied alloys with values between 70 and 90 GPa, which are lower than those of the commercial alloys used in load transfer bone implants.

Keywords low elastic modulus, nanoindentation, Ni-free Ti alloys, shape memory effect

1. Introduction

Shape memory effect (SME) refers to the ability of certain materials to recover a predetermined shape when heated or stressed (Ref 1, 2). This ability is due to a reversible solid-state phase transformation from austenite (β-phase) to martensite (α″-phase). The shape memory alloys exhibit a number of remarkable properties such as shape memory effect, superelasticity, high damping capacity, low elastic modulus, and wear resistance (Ref 1-3). These properties make them promising candidates for biomedical applications such as prosthesis, osteosynthesis plates and screws, and orthodontic wires. Furthermore, such alloys present excellent corrosion resistance and biocompatibility (Ref 4). NiTi alloys are the only shape memory alloys which have been used as implantable materials in the human body (Ref 5).

However, Ni ions released from the implant to the surrounding tissue produces adverse reactions such as allergy, which affects up to 20% of women (Ref 6, 7). There are two main ways to solve the problem: the surface modification treatments such as oxidizing to reduce Ni surface concentration (Ref 8) and the design of new Ni-free Ti alloys (Ref 9-11).

The most commercial alloys used as implant materials present elastic modulus in the range of 110 to 220 GPa from Ti and Co-Cr-Mo alloys. A lower elastic modulus, near to that of cortical bone (25 GPa) (Ref 12), is required in order to decrease the stress-shielding effect and to enhance bone remodeling (Ref 13). Current research is specially focusing on new β-type Ti alloys, using β-stabilizing alloying elements such as Nb, Ta, Zr, and Hf, which exhibit lower elastic modulus and possible martensitic transformation.

In 1988, Morinaga and co-workers (Ref 14) introduced a theoretical method based on molecular orbitals for designing Ti-alloys with a significant reduction in terms of both time and cost. The purpose of this method is to consider the effect of alloying elements for predicting the stable phase of Ti-alloys based on phase stability maps as functions of two quantum parameters: the bond order (Bo) and the d-orbital energy level (Md). Bo represents the covalent bond strength between Ti and the alloying element, and Md is correlated with the electronegativity and metallic radius of the element.

The aim of this study is to achieve a material with shape memory properties and/or low elastic modulus to be used in load transfer implantology. For this purpose, three new Ni-free Ti alloys were designed and produced using the new properties map based on the abovementioned theoretical method for decreasing time and experimentation cost. Finally, the alloys were microstructurally and mechanically characterized.

2. Experimental

A theoretical method based on molecular orbitals was used to predict the stable phase and design three new Ti alloys (Ref 15). The method consists on the creation of a new map based on two quantum parameters, Bo and Md, calculated by the implementation of Khon-Sham from the Density Functional

This article is an invited paper selected from presentations at Shape Memory and Superelastic Technologies 2008, held September 21-25, 2008, in Stressa, Italy, and has been expanded from the original presentation.

M. González, J. Peña, J.M. Manero, M. Arciniegas, and **F.J. Gil**, Department of Materials Science and Metallurgy, Universitat Politècnica de Catalunya, Avda. Diagonal 647, Barcelona 08028, Spain; and **J. Peña**, Materials Science, Elisava Escola Superior de Disseny, C/Ample 11-13, Barcelona 08002, Spain. Contact e-mails: Marta.Gonzalez.Colominas@upc.edu, jpenya@elisava.es, Jose.Maria.Manero@upc.edu, Milena.Arcienagas@upc.edu, Francesc.Xavier.Gil@upc.edu.

Theory (DFT) (Ref 16) and based on a database of 132 alloys. The application of the resulting parameters to the data base permitted to build a new phase stability map in which two zones can be distinguished, delimited by the dot and dashed line corresponding to the probability to obtain a low elastic modulus and the shape memory effect, respectively. Three pairs of $(\overline{Bo}, \overline{Md})$, were selected on the β-zone, in the frontier between the low elastic modulus and the shape memory effect, in order to study a new system and a new zone of the design map (Fig. 1). The compositions were determined by using Nb, Hf, and Zr as alloying elements and are listed in Table 1.

The determination of β-transus temperature and Mo equivalent was carried out by using Eq 1 and 2, respectively, in order to design the heat treatment (Ref 17). The β-transus for pure Ti is reported as 882 °C and the addition of β-stabilizing solutes reduces this value.

$$T_{\beta\text{transusalloy}} = T_{\beta\text{transusTi}} - 7.22\,\text{wt.\%\,Nb} \quad \text{(Eq 1)}$$

$$[\text{Mo}]_{\text{eq}} = 0.28\,\text{wt.\%\,Nb} \quad \text{(Eq 2)}$$

A 40 g button of each alloy was made by vacuum arc melting, using high purity (99.99%) starting elemental materials. The buttons were sealed under vacuum into a quartz capsule, homogenized at 1100 °C for 12 h, solution treated at 1100 °C for 1.5 h and then quenched in ice water. The samples were mechanically polished and finished with colloidal silica to give a surface roughness with a Ra < 100 nm. The chemical composition was verified by x-ray fluorescence using Philips PW2400 equipment. Optical microstructural analysis was carried out after Keller reactive attack (2 mL HF, 3 mL HCl, 5 mL HNO_3, and 190 mL distilled H_2O). Thin disks of 3-mm diameter were electropolished for transmission electron microscopy (TEM) in an electrolyte consisting of 400 mL butoxyethanol, 400 mL methanol, and 100 mL perchloric acid.

Differential scanning calorimetry studies were carried out on a DSC Q1000 TA Instrument. Two entire heating-cooling cycles from −90 to 200 °C at a heating and cooling rate of 10 °C/min were used to investigate the presence of martensitic transformation and that of in thermoelastic martensitic transformation.

Finally, nanoindentation tests were conducted using a MTS Nano Indenter XP with Continuous Stiffness Measurement (CSM) module. Elastic modulus was measured from monotonic load tests to a depth of 2000 nm using a Berkovich tip with a measured radius of 750 nm. Data have been analyzed using the Oliver and Pharr method (Ref 18, 19). Furthermore, cyclic nanoindentation tests to a depth of 2000 nm were developed

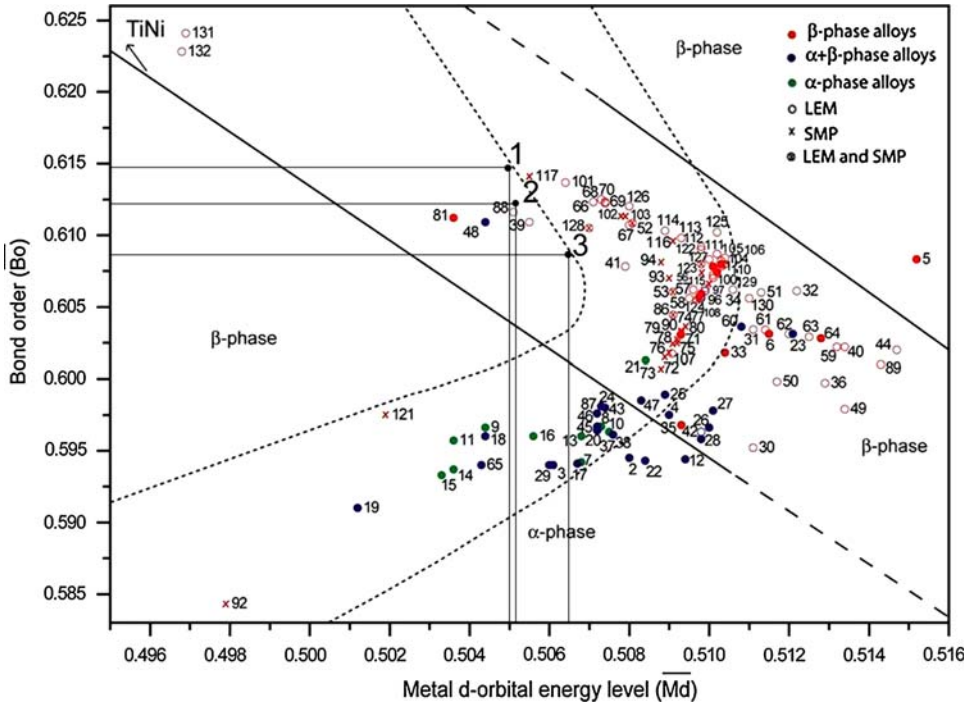

Fig. 1 Design map based on two quantum parameters, Bo and Md

Table 1 Relevant properties of the three new alloys: chemical composition (wt.%), microstructure, grain-size, β-transus temperature, Mo equivalent, thermoelastic phase transformation (TPT), and elastic modulus calculated by using a Berkovich tip (GPa)

Chemical composition, wt.%	No.	Microstructure	Grain-∅, μm	β-transus, °C	Mo eq.	TPT	*E*, Gpa
Ti-16.2Hf-24.8Nb-1Zr	1	β + α″	900 ± 482	709	6.7	Yes	74 ± 1.5
Ti-5.2Hf-31.2Nb-0.4Zr	2	β + α′	850 ± 492	658	8.7	No	76 ± 4
Ti-16Hf-36.2Nb-1Zr	3	β	525 ± 178	629	9.8	No	91 ± 2

using a spherical tip of radius 25 μm for evidencing the martensitic thermoelastic phase transformation from the load-displacement curves.

3. Results and Discussion

The relevant properties of the microstructural and mechanical characterization of the three new alloys are shown in Table 1.

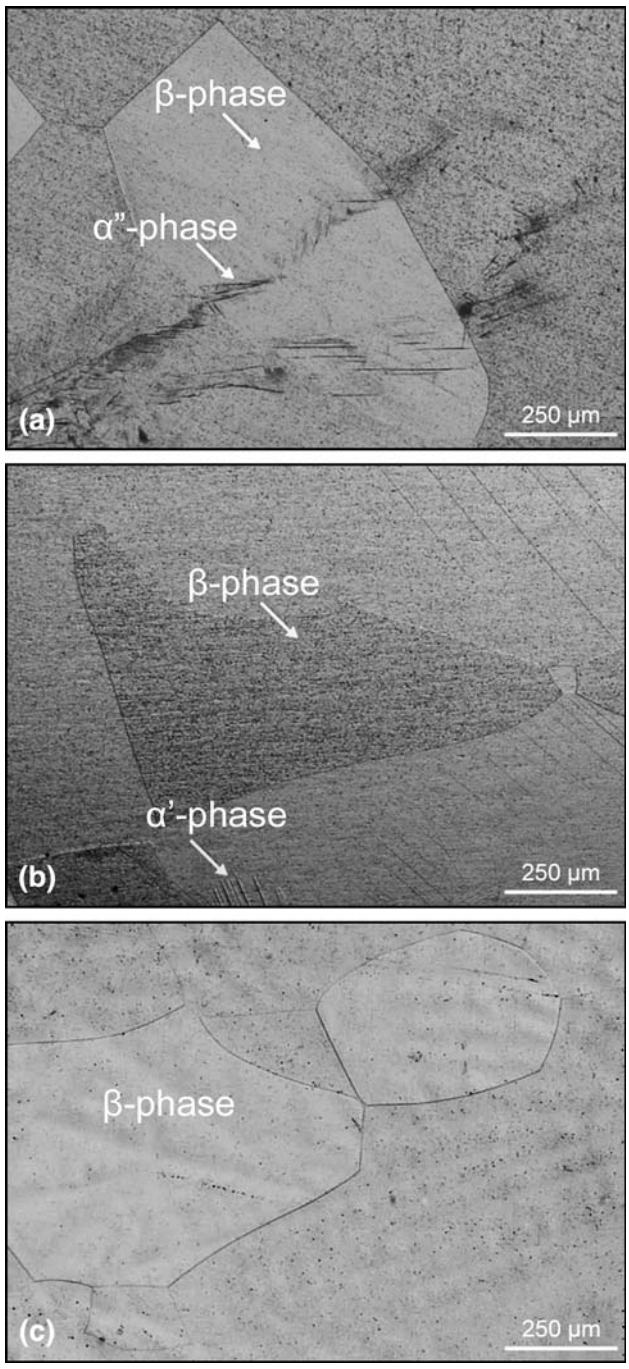

Fig. 2 Optical microscopy images of the alloys numbered as 1 (a), 2 (b), and 3 (c)

A notable decrease of β-transus temperature as a function of Mo equivalent was observed in the studied alloys. Heat treatment could be done at lower temperature which would reduce the average grain size.

As it was expected, because of the high content of β-stabilizing elements mainly β-phase was observed in the new alloys with a size range of 525 to 900 μm (Fig. 2). Moreover, small areas with fine orthorhombic martensitic plates nucleated from grain boundaries were observed in the alloys number 2 and 3.

X-ray diffraction results confirmed the presence of β-phase in the three alloys associated with (110), and (200) diffraction peaks and two low peaks associated with (013) and (131), indexed as α″-phase. In alloys numbered as 2, α′ peaks were detected associated with the (110) and (211) diffraction planes. In alloy number 3, with the higher Mo equivalent, only β-phase was observed (Fig. 3). The results confirmed that the presence of martensitic phase is conditioned by the β-stabilizer content.

The DSC patterns obtained from the three alloys did not evidence any martensitic transformation. This fact can be due to the low enthalpy values reported for the Ni-free Ti alloys (Ref 20).

However, the images obtained by TEM showed the presence of α″ martensite plates which got re-oriented and disappeared when increasing the intensity of the electron current beam (Fig. 4). This means that the heat produced by the electron beam induced the martensitic transformation from the austenitic phase, justifying the reversibility of the transformation (thermoelastic transformation).

In order to obtain more details about the martensitic transformation of alloy 1, TEM analysis was repeated by using an electron microscope with temperature control unit. The test started at 0 kV corresponding to 0 °C temperature. In this condition, the alloy presented a microstructure formed by martensitic plates inside the β-matrix (Fig. 5a). At 0.40 kV, corresponding to 60 °C, the complete transformation from martensite (α″) to austenite (β) was observed (Fig. 5b).

The elastic modulus of the three alloys (between 74 and 91 GPa) was lower than those presented by the commercial alloys used as load transfer implant materials. Moreover, the

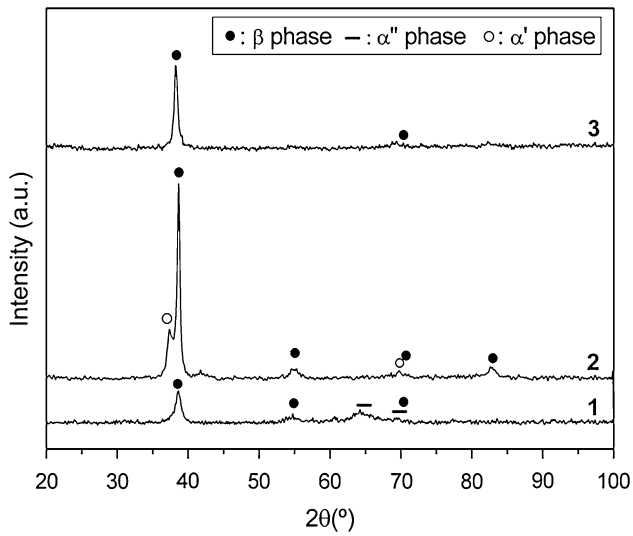

Fig. 3 X-ray diffraction patterns of the three new alloys

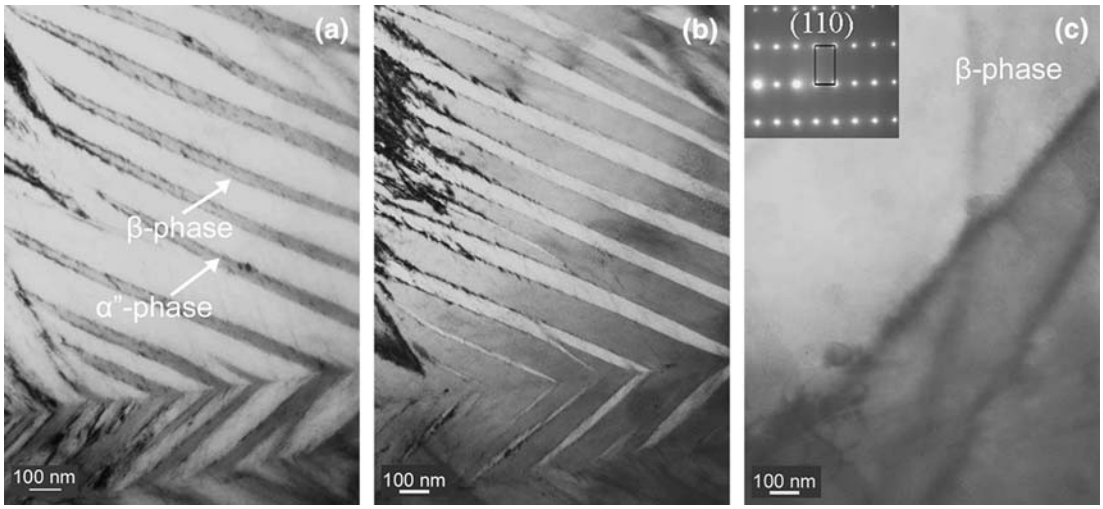

Fig. 4 Bright-field TEM image of the alloy number 1 at low (a), medium (b), and high (c) electron current beam intensity

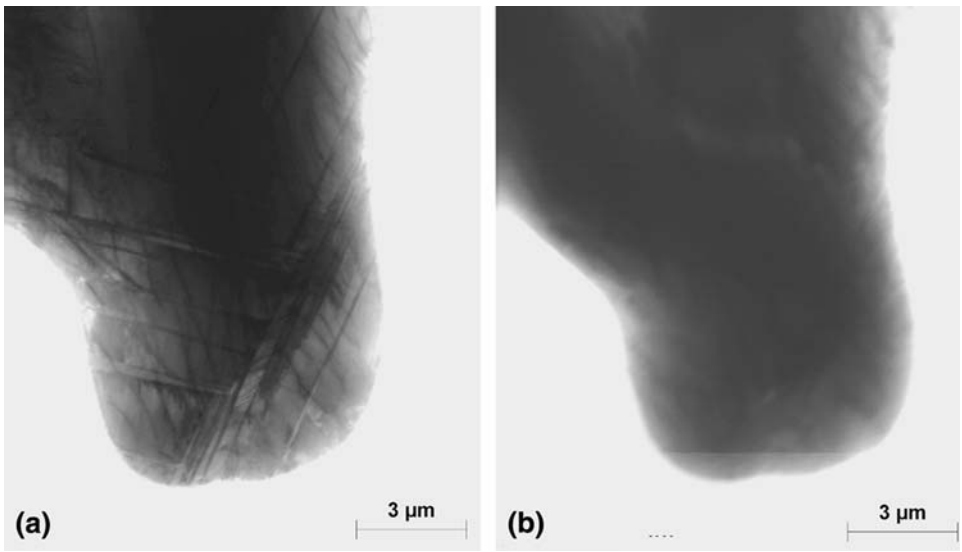

Fig. 5 Bright-field TEM image of the alloy number 1 at 0 kV (a) and 0.40 kV (b)

lowest elastic modulus corresponded to alloy number 1, which also presented thermoelastic martensitic transformation observed by TEM.

Finally, Fig. 6 shows one representative load-displacement curve of each alloy obtained by cyclic nanoindentation tests to a depth of 2000 nm. Load-displacement curve of alloy number 1 (Fig. 6a) evidenced a discontinuity on the loading portion reported as pop-in from the fourth loading-unloading cycle. A pop-in is characterized by the increase of the applied load without the consequent increase in the contact stress as a mechanism of deformation accommodation (Ref 21). Hysteresis loops generated between the unloading and the re-loading curves are especially observed after the appearance of the first pop-in in the fourth cycle. In transforming materials, when load is released, the elastic response and the reverse phase transformation contribute to the recovery, causing the observed loops. Both events pop-in and hysteresis loops of the alloy numbered as 1, are associated with the martensitic transformation. On the other hand, as it was expected, alloys number 2 and 3 did not evidence changes on the loading curve and neither hysteresis loops, indicating that thermoelastic martensitic transformation did not take place in that alloys (Fig. 6b, c).

Alloy numbered as 2, also showed the presence of martensitic plates, which remained stable when increasing the current electron beam intensity (Fig. 7).

4. Conclusions

The following conclusions can be drawn from this study:

Three new Ni-free Ti alloys were designed by implementing a new design method. From the obtained results it was verified the utility of the method in the studied zone.

The results showed a low elastic modulus in the three new alloys, lower than those presented by the commercial alloys used as load transfer implant materials.

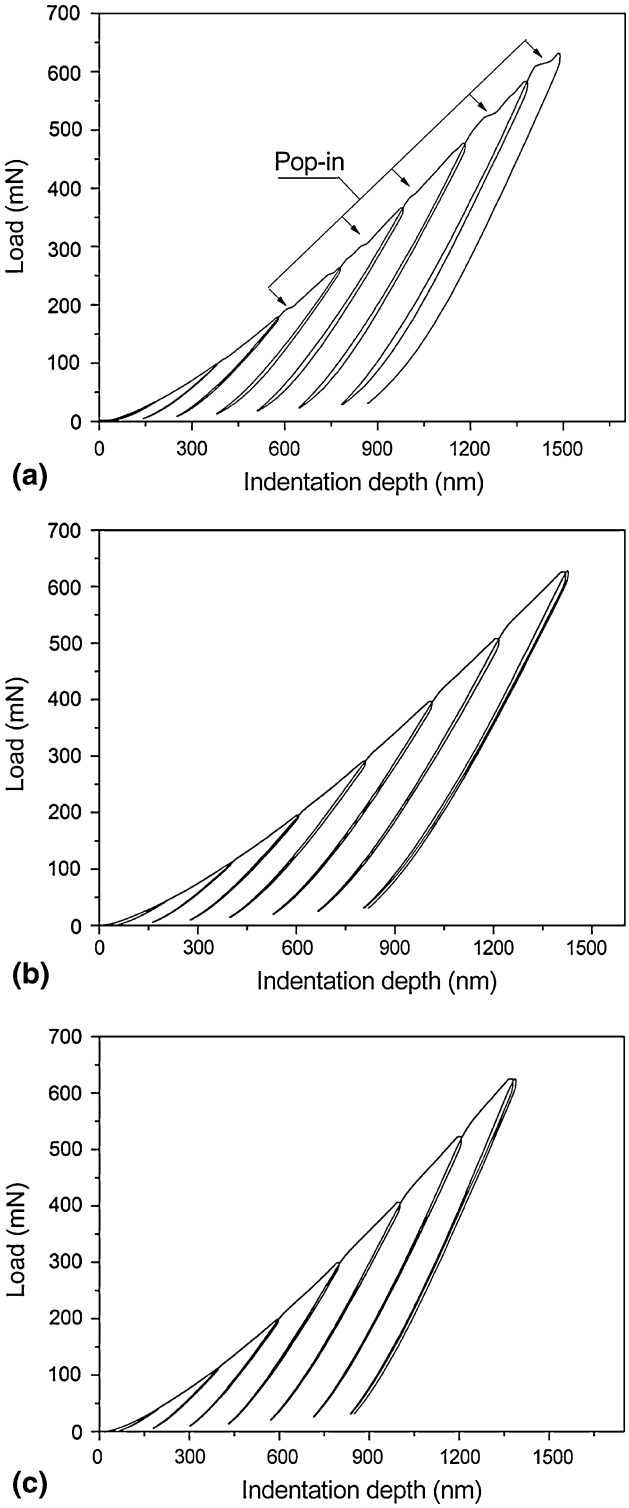

Fig. 6 Cyclic nanoindentation load-displacement curves of the alloys numbered as 1 (a), 2 (b), and 3 (c)

TEM images and also pop-in event and hysteresis loops observed on the alloy numbered as 1 were indicative that the alloy presented thermoelastic martensitic transformation. It is worth highlighting that the low elastic modulus of alloy number 1, with 74 GPa, also presented thermoelastic martensitic transformation observed by TEM and cyclic nanoindentation using a spherical tip.

Fig. 7 Bright-field TEM image of the alloy number 2

However, the results of alloy number 1 should be optimized by thermomechanical treatments.

Acknowledgments

With the support of the Generalitat de Catalunya Commission for the Universities and Research of the Department of Innovation, Universities and Companies and the European Social Fund.

References

1. T.W. Duerig, K.N. Melton, D. Stoeckel, and C.M. Wayman, *Engineering Aspects of Shape Memory Alloys*, Butterworth-Heinemann Ltd., London, 1990
2. T.W. Duering and A.R. Pelton, Ti-Ni Shape Memory Alloys, in *Materials Properties Handbook Titanium Alloys*, R. Boyer, G. Welsch, and E.W. Collings, Eds., ASM International, Materials Park, OH, 1994, p 1035
3. K. Otsuka and C.M. Wayman, Eds., *Shape Memory Materials*, University of Illinois, Urbana-Champaign, 1999
4. G. Rondelli, Corrosion Resistance Tests on NiTi Shape Memory Alloy, *Biomaterials*, 1996, **17**(20), p 2003–2008
5. C.D.J. Barras and K.A. Myers, Nitinol—Its Use in Vascular Surgery and Other Applications, *Eur. J. Vasc. Endovasc. Surg.*, 2000, **19**(6), p 564–569
6. G.C. McKay, R. Macnair, C. MacDonald, and M.H. Grant, Interactions of Orthopaedic Metals with an Immortalized Rat Osteoblast Cell Line, *Biomaterials*, 1996, **17**(13), p 1339–1344
7. H. Kerosuo, A. Kullaa, E. Kerosuo, L. Kanerva, and A. Hensten-Pettersen, Nickel Allergy in Adolescents in Relation to Orthodontic Treatment and Piercing of Ears, *Am. J. Orthod. Dentofacial Orthop.*, 1996, **109**(2), p 148–154
8. A. Michiardi, C. Aparicio, J.A. Planell, and F.J. Gil, Electrochemical Behaviour of Oxidized NiTi Shape Memory Alloys for Biomedical Applications, *Surf. Coat. Technol.*, 2007, **201**(14), p 6484–6488
9. K. Nitta, S. Watanabe, N. Masahashi, H. Hosada, and S. Hanawa, *Symposium on Structural Biomaterials for the 21st Century*, M. Niinomi, T. Okabe, E.M. Taleff, D.R. Lesuer, and H.F. Lippard, Eds., TMS, 2001, p 25–34
10. D. Kuroda, M. Niinomi, M. Morinaga, Y. Kato, and T. Yashiro, Design and Mechanical Properties of New β Type Titanium Alloys for Implant Materials, *Mater. Sci. Eng. A*, 1998, **243**(1–2), p 244–249

11. E. Takahashi, S. Watanabe, and S. Hanada, *Proceedings of the International Conference on Shape Memory and Superelastic Technologies*, USA, 2003, p 91–99
12. J.-Y. Rho, T.Y. Tsui, and G.M. Pharr, Elastic Properties of Human Cortical and Trabecular Lamellar Bone Measured by Nanoindentation, *Biomaterials*, 1997, **18**(20), p 1325–1330
13. M. Niinomi, Recent Research and Development in Titanium Alloys for Biomedical Applications and Healthcare Goods, *Sci. Technol. Adv. Mater.*, 2003, **4**(5), p 445–454
14. M. Morinaga, M. Kato, T. Kamimura, M. Fukumoto, I. Harada, and K. Kubo, *Sixth World Conference on Titanium*, France, 1, 1988, p 1601
15. M. Arciniegas, J.M. Manero, J. Peña, F.J. Gil, and J.A. Planell, Study of New Multifunctional Shape Memory and Low Elastic Modulus Ni-Free Ti Alloys, *Metall. Mater. Trans. A*, 2008, **39**(4), p 742–751
16. P.J. Hay and W.R. Wadt, Ab Initio Effective Core Potentials for Molecular Calculations Potentials for the Transition Metal Atoms Sc to Hg, *J. Chem. Phys.*, 1985, **82**, p 270
17. R. Boyer, G. Welsch, and E.W. Collings, *Materials Properties Handbook: Titanium Alloys*, ASM International, Materials Park, OH, 1998, p 5–11
18. A.C. Fischer-Cripps, *Nanoindentation*, 2nd ed., Springer, New York, 2004, p 16–45
19. G.M. Pharr, Measurement of Mechanical Properties by Ultra-low Load Indentation, *Mater. Sci. Eng. A*, 1998, **253**(1–2), p 151–159
20. Y.L. Hao, S.J. Li, S.Y. Sun, and R. Yang, Effect of Zr and Sn on Young's Modulus and Superelasticity of Ti-Nb-based Alloys, *Mater. Sci. Eng. A*, 2006, **441**(1–2), p 112–118
21. S. Bhagavat and I. Kao, Nanoindentation of Lithium Niobate: Hardness Anisotropy and Pop-in Phenomenon, *Mater. Sci. Eng. A*, 2005, **393**(1–2), p 327–331